S-^{11}C-Methyl-L-Cysteine: A New Amino Acid PET Tracer for Cancer Imaging

Huaifu Deng[1,2], Xiaolan Tang[3], Hongliang Wang[1], Ganghua Tang[1], Fuhua Wen[1], Xinchong Shi[1], Chang Yi[1], Kening Wu[1], and Quanfei Meng[2]

[1]PET-CT Center, Department of Nuclear Medicine, First Affiliated Hospital, Sun Yat-Sen University, Guangzhou, China; [2]Department of Radiology, First Affiliated Hospital, Sun Yat-Sen University, Guangzhou, China; and [3]Department of Applied Chemistry, South China Agricultural University, Guangzhou 510642, China

S-^{11}C-methyl-L-cysteine (^{11}C-MCYS), an analog of *S*-^{11}C-methyl-L-methionine (^{11}C-MET), can potentially serve as an amino acid PET tracer for tumor imaging. The aim of this study was to investigate the radiosynthesis and perform a biologic evaluation of ^{11}C-MCYS as a tumor imaging tracer. The results of the first human PET study are reported. **Methods:** ^{11}C-MCYS was prepared by ^{11}C-methylation of the precursor L-cysteine with $^{11}CH_3I$ and purification on commercial C18 cartridges. In vitro competitive inhibition experiments were performed with Hepa1–6 hepatoma cell lines, and biodistribution of ^{11}C-MCYS was determined in normal mice. The incorporation of ^{11}C-MCYS into tissue proteins was investigated. In vivo ^{11}C-MCYS uptake studies were performed on hepatocellular carcinoma–bearing nude mice and inflammation models and compared with ^{11}C-MET PET and ^{18}F-FDG PET. In a human PET study, a patient with a recurrence of glioma after surgery was examined with ^{11}C-MCYS PET and ^{18}F-FDG PET. **Results:** The uncorrected radiochemical yield of ^{11}C-MCYS from $^{11}CH_3I$ was more than 50% with a synthesis time of 2 min, the radiochemical purity of ^{11}C-MCYS was more than 99%, and the enantiomeric purity was more than 90%. In vitro studies showed that ^{11}C-MCYS transport was mediated through transport system L. Biodistribution studies demonstrated high uptake of ^{11}C-MCYS in the liver, stomach wall, and heart and low uptake of ^{11}C-MCYS in the brain. There was higher accumulation of ^{11}C-MCYS in the tumor than in the muscles. The tumor-to-muscle and inflammatory lesion–to–muscle ratios were 7.27 and 1.62, respectively, for ^{11}C-MCYS, 5.08 and 3.88, respectively, for ^{18}F-FDG, and 4.26 and 2.28, respectively, for ^{11}C-MET at 60 min after injection. Almost no ^{11}C-MCYS was incorporated into proteins. For the patient PET study, high uptake of ^{11}C-MCYS with true-positive results, but low uptake of ^{18}F-FDG with false-negative results, was found in the recurrent glioma. **Conclusion:** Automated synthesis of ^{11}C-MCYS is easy to perform. ^{11}C-MCYS is superior to ^{11}C-MET and ^{18}F-FDG in the differentiation of tumor from inflammation and seems to have potential as an oncologic PET tracer for the diagnosis of solid tumors.

Key Words: $^{11}CH_3I$; *S*-^{11}C-methyl-L-cysteine; amino acid; tumor; inflammation; PET imaging

J Nucl Med 2011; 52:287–293
DOI: 10.2967/jnumed.110.081349

As a glucose metabolism tracer, ^{18}F-FDG has been widely used in PET imaging for oncology and treatment evaluation (*1*). However, clinical ^{18}F-FDG PET studies have demonstrated several limitations, such as difficulty in differentiating tumor from inflammation because of high uptake of ^{18}F-FDG in tumors and in nonmalignant inflammatory tissue (*2*), thus motivating efforts to develop new oncologic PET tracers. Positron-labeled amino acids have proven to be useful for imaging tumors, especially brain tumors and peripheral tumors such as those in the lung, breast, and liver and lymphomas. Currently, *S*-^{11}C-methyl-L-methionine (^{11}C-MET) is the most commonly used amino acid tracer for tumor imaging with PET (*3*). However, some investigations, including many clinical PET studies, have shown that increased ^{11}C-MET uptake is not specific to malignant tumors (*4–6*). ^{11}C-MET is also taken up in some inflammatory lesions (*7*). It has been reported that ^{11}C-MET is incorporated not only into protein fractions via the conversion into amino-acyl-transfer RNA but also into nonprotein materials, such as phospholipids and RNA, by the transmethylation process via *S*-adenosyl-L-methionine (*8*), making correct quantitative investigation difficult. Because of the short half-life of ^{11}C, many ^{18}F-labeled amino acids have been developed. Among them, *O*-2-^{18}F-fluoroethyl-L-tyrosine (^{18}F-FET) is another commonly used amino acid tracer for the detection of tumors and has been superior to ^{18}F-FDG in distinguishing tumors from inflammation (*9*). However, the automated radiosynthesis of ^{18}F-FET with complex high-performance liquid chromatography purification is cumbersome and time-consuming (*10*), compared with the production of ^{11}C-MET by on-column methylation (*11*). Thus, the easy availability of ^{11}C-methyl–containing tracers in the PET center with an in-house cyclotron gives them potential for use in clinical PET.

S-^{11}C-methyl-L-cysteine (^{11}C-MCYS), an analog of ^{11}C-MET, has not been evaluated as a tumor imaging agent. In

Received Jul. 16, 2010; revision accepted Nov. 18, 2010.
For correspondence or reprints contact either of the following:
Ganghua Tang, PET-CT Center, Department of Nuclear Medicine, The First Affiliated Hospital, Sun Yat-Sen University, Guangzhou 510080, China.
E-mail: gtang0224@yahoo.com.cn
Quanfei Meng, Department of Radiology, The First Affiliated Hospital, Sun Yat-Sen University, Guangzhou 510080, China.
E-mail: cjr.mengquanfei@vip163.com

this work, we report the easy-to-automate radiosynthesis and perform a biologic evaluation of ^{11}C-MCYS as a malignant tumor tracer more specific than ^{18}F-FDG and ^{11}C-MET. In addition, the first ^{11}C-MCYS PET study on a patient is reported.

MATERIALS AND METHODS

Chemicals

All reagents used in the synthesis were commercial products applied without further purification unless otherwise indicated. Acetonitrile, dimethylsulfoxide, *N,N*-dimethylformamide, tetrahydrofuran, lithium aluminum hydride (1.0 M in tetrahydrofuran), hydroiodic acid, and L-cysteine were purchased from Sigma-Aldrich.

Cell Culture

A hepatocellular carcinoma cell line (Hepa1–6) was obtained from the Laboratory Animal Center of Sun Yat-Sen University, Guangzhou, China. The cells were cultivated in RPMI 1640 medium with a physiologic glucose concentration (1.0 g/L) containing 5% fetal calf serum at 37°C in a humidified atmosphere of 5% CO_2 and 95% air. The medium was routinely renewed 3 times a week. Two days before the in vitro experiments, the cells were trypsinized and 2×10^5 cells per well were seeded into 24-well plates.

Animals and Tumors

Female and male C57BL/6J mice (6 wk old) were obtained from the Laboratory Animal Center of Sun Yat-Sen University. Mice and nude mice were housed 5 animals per cage under standard laboratory conditions at 25°C and 50% humidity. They were allowed free access to food and water. We prepared 3 groups of mice, namely normal mice ($n = 30$), tumor nude mice ($n = 20$), and inflammation mice ($n = 20$). Tumor nude mice were inoculated subcutaneously in the femoral region with 1.0×10^7 Hepa1–6 cells. Inflammation mice were inoculated subcutaneously with 0.2 mL of turpentine oil (Wako Chemical) (*12*). These turpentine-induced masses showed acute inflammation histologically as described in an earlier report (*13*). All animals were kept in cages under standardized conditions. At the time of the experiments, the mice were 9–10 wk old and weighed 18–25 g. The mass of the tumors and inflammatory tissue grew to 10–25 mm during the experiments. The study was performed according to the guidelines and recommendations of the Committee on Animal and Human Research at the First Affiliated Hospital, Sun Yat-Sen University. The protocol was fully approved by the local institutional review committee on animal care.

Radiosynthesis Procedures

$^{11}CO_2$ was produced by $^{14}N(p,\alpha)^{11}C$ nuclear reactions using a Cyclone 10/5 cyclotron (IBA) and was delivered to the radiochemical laboratory. $^{11}CO_2$ was trapped in a loop ring cooled at –160°C with liquid nitrogen. After a flush with helium, the ring was warmed and $^{11}CO_2$ released into the reactor module under a helium flow (20 mL/min), through a dehydrating agent, P_2O_5. $^{11}CH_3I$ was produced through reduction of $^{11}CO_2$ with $LiAlH_4$, hydrolysis of the intermediately formed organometallic complex, and subsequent iodination of ^{11}C-methanol with hydrogen iodide. ^{11}C-MCYS were synthesized according to the solid-phase ^{11}C-methylation of the precursor L-cysteine loaded into a C18 column with $^{11}CH_3I$ (Fig. 1). Briefly, $^{11}CH_3I$ produced as described above was delivered under a helium flow (20 mL/min) to a Sep-Pak Plus C18 cartridge (Waters) previously loaded with a solution of

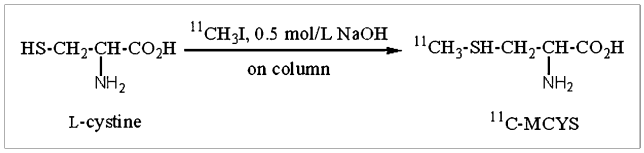

FIGURE 1. Radiosynthesis of ^{11}C-MCYS by on-column ^{11}C-methylation of L-cysteine.

L-cysteine (~2 to 3 mg) dissolved in NaOH 0.5 mol/L in 50:50 ethanol:water (v/v, 0.210 mL). ^{11}C-MCYS was eluted with NaH_2PO_4 0.05 M buffer (5 mL, pH ~3 to 4) and collected in a vented sterile vial. The solution was finally sterilized by a 0.22-mm filter to give the final formulation. The fully automated synthesis of ^{11}C-MCYS was performed on a simple, remotely controlled commercial ^{11}C-methylation module (PET-CS-I-IT-I ^{11}C-methylation synthesizer; PET (Beijing) Technology Co., Ltd.) as shown in Supplemental Figure 1 (supplemental materials are available online only at http://jnm.snmjournals.org).

^{11}C-MET and ^{18}F-FDG were synthesized as published previously by Tang et al. (*14,15*).

Quality Control Procedures

Radiochemical purity and chemical purity of ^{11}C-MCYS were measured by analytic high-performance liquid chromatography with an Eclipse XDB-C18 analytic column (4.6 × 150 mm, 5 μm; Agilent) using 55:45 CH_3OH:3 mM NaH_2PO_4 (v/v) as the mobile phase at a flow rate of 1 mL/min. The elution was monitored by an ultraviolet detector (254 nm) and radiodetector. The pH was measured by a standard pH meter. Absence of pyrogen in the injectable solutions was checked by limulus amebocyte lysate testing using a gel clotting assay, and samples were tested for sterility.

Transport Assays

Transport assays with Hep1–6 cells were performed at 2 d after seeding during the exponential growth phase. The method of measuring transport was similar to a method reported previously (*2,16,17*). The competitive inhibition experiments to characterize the transport system were performed in the presence of the specific competitive inhibitors: for system L, 2′-aminobicyclo(*2,2,1*)-heptane-2′-carboxylic acid (BCH); for system A, *N*-methylamino-isobutyric acid (MeAIB); and for system ASC, MeAIB plus serine. The concentration of the inhibitors used was 15 mmol/L. Parallel experiments with increasing concentrations of MCYS were performed to investigate the capacity of the transport system. All experiments were performed in the presence and absence of Na^+. In Na^+-free experiments, sodium salts were replaced by choline chloride. Each experiment was done in triplicate and averaged and was repeated 5 times on different days. After preincubation of the cells in 200 μL of the medium for 30 min, 200 μL of ^{11}C-MCYS (1.85 MBq/mL) and 200 μL of one of the inhibitors or MCYS (50, 100, 200, 300, or 350 μmol/L) were added and samples were incubated at 37°C for 4 min. After tracer uptake had been stopped with 1 mL of ice-cold 1× phosphate-buffered saline, the cells were washed 3 times with phosphate-buffered saline at 4°C and dissolved in 1.5 mL of 0.1 M NaOH plus 2% Triton X (Sigma Chemical Co.) and the activity measured by a γ-counter.

In Vivo Biodistribution Studies

The animals were anesthetized with pentobarbital (75 mg/kg) before injection of radiotracer and remained anesthetized through the study. They were injected with 0.74–1.48 MBq (20–40 μCi) of

radiotracer in 100–200 μL of saline through the tail vein (^{11}C-MCYS and ^{11}C-MET in phosphate-buffered saline and ^{18}F-FDG in normal saline). A prescribed duration was allowed before procurement of organs and tissues. Blood was obtained through the eyeball, tissue samples of interest (blood, brain, heart, lung, liver, kidney, and small intestine in normal mice) were rapidly dissected and weighed, and ^{11}C radioactivity was counted with an automatic γ-counter. All measurements were background-subtracted and decay-corrected to the time of killing and then averaged (*2*). Data were expressed as a percentage of the injected dose per gram of tissue (%ID/g).

Incorporation of ^{11}C-MCYS into Proteins

To determine the extent of protein incorporation of ^{11}C-MCYS, protein-bound activity in the brain, pancreas, tumor, and blood samples was determined at 30 min after injection. For this purpose, tumor, pancreatic, and cerebral tissue (~50 to 100 mg in wet weight) was homogenized by the addition of 1 mL of distilled water and by ultrasonication at 0°C. Blood samples were immediately centrifuged at 4,000*g,* and 250 μL of 50% trichloroacetic acid were added to 750 μL of plasma and stirred in a vortex mixer for 1 min. After centrifugation, the supernatants were removed from the pellets. The radioactivity in the acid solution and acid-precipitable fraction was measured with a γ-counter. Sampling of the ^{11}C-activity was performed using the supernatant solution after spiking with a small amount of MCYS by high-performance liquid chromatography (55:45 CH_3OH:3 mM NaH_2PO_4 (v/v)), and the elution profile was detected with an ultraviolet detector at 254 nm. Incorporation of ^{11}C-MCYS into tumor, pancreatic, and cerebral tissue was measured as described. Radioactivities contained in the acid solution (supernatant solution) and acid-precipitable fraction (protein pellet) were also determined.

PET Studies

PET was performed using a Gemini GXL scanner (Philips). Before undergoing ^{11}C-MCYS, ^{11}C-MET, and ^{18}F-FDG PET studies, the animals were kept fasting for at least 4 h. The tumor-bearing mice and inflammation model mice were anesthetized with pentobarbital (75 mg/kg) before injection of the radiotracer and remained anesthetized throughout the study. ^{11}C-MCYS, ^{11}C-MET, or ^{18}F-FDG (10 MBq) was injected in 100–200 μL of phosphate-buffered saline or normal saline through the tail vein. Then, image acquisition was performed at 60 min after intravenous injection in 3-dimensional mode, with emission scans of 4 min per bed position. Imaging started with a low-dose CT scan (30 mAs), immediately followed by a PET scan. The CT scan was used for attenuation correction and localization of the lesion site. In addition, a 45-y-old patient with a history of attempted resection of grade IV glioma 1 y previously was also examined with ^{18}F-FDG and ^{11}C-MCYS PET. The coronal, transaxial, and sagittal PET views of tumor-bearing mice, inflammation model mice, and the patient were obtained after image reconstruction with a slice thickness of 2.0 mm. A region of interest was placed on each tumor, each inflammatory lesion, and a region of femoral muscle. The human study was approved by the Institutional Review Board of the First Affiliated Hospital, Sun Yat-Sen University. Informed consent was obtained from the patient before injection.

Statistical Analysis

Statistical analysis was performed with SPSS software, version 15.0 (SPSS Inc.), for Windows (Microsoft). All data were expressed as mean ± SD. Comparisons between conditions were performed using the unpaired, 2-tailed Student *t* test. A *P* value of less than 0.05 was considered to indicate statistical significance.

RESULTS

Radiosynthesis Results

The uncorrected radiochemical yield of $^{11}CH_3I$ was 60%–70% from $^{11}CO_2$, and the synthesis time was 8–10 min after release of $^{11}CO_2$. The uncorrected radiochemical yield of ^{11}C-MCYS from $^{11}CH_3I$ was more than 50% with a synthesis time of 2 min. The radiochemical purity of ^{11}C-MCYS was more than 99% (Fig. 2), the enantiomeric purity was more than 90%, and the total synthesis time from $^{11}CO_2$ was about 12 min. The retention time was approximately 1.8–2.2 min for ^{11}C-MCYS, less than 1.5 min for cysteine, and approximately 5.8–6.5 min for $^{11}CH_3I$. ^{11}C-MET was synthesized with high chemical and radiochemical purity (*13*).

Transport Mechanism of ^{11}C-MCYS In Vitro

In the competitive inhibition experiments, the specific transport inhibitors BCH, MeAIB, and MeAIB plus serine were used to inhibit the 3 main transport systems of ^{11}C-MCYS. The addition of BCH, specific for system L, resulted in an approximately 80% reduction of ^{11}C-MCYS uptake, whereas the addition of MeAIB and MeAIB plus serine, specific for systems A and ASC, caused no significant change ($P = 0.19$) in tracer uptake (Fig. 3A). Therefore, a specific transport of ^{11}C-MCYS in Hep1–6 cells was mediated mainly by system L, and almost no involvement of systems A and ASC could be demonstrated. To clarify the character of the transport system, we examined the Na^+ dependency of ^{11}C-MCYS uptake. Uptake of ^{11}C-MCYS was not affected by the presence of Na^+ ions. Figure 3 shows the inhibition of Na^+-independent amino acid transporters involved in the uptake of ^{11}C-MCYS. The experiments with increasing concentrations of MCYS (0–400 μmol/L) showed no significant change in the radioactivity concentration in the cells (Fig. 3B). No saturation of transport capacity was found until a concentration of 350 μmol/L had been reached.

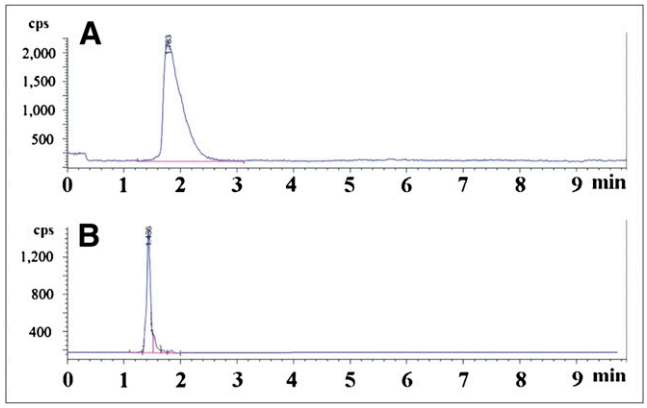

FIGURE 2. Typical high-performance liquid chromatograms of ^{11}C-MCYS and standard coinjection: radioactive chromatogram of ^{11}C-MCYS (A) and ultraviolet chromatogram of standard MCYS (B).

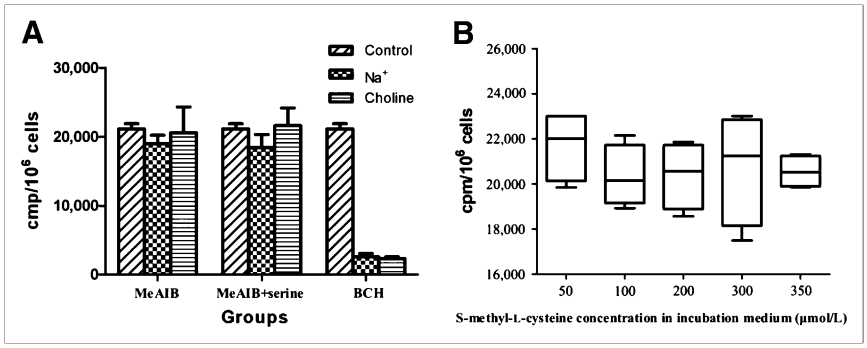

FIGURE 3. (A) Uptake of ^{11}C-MCYS per 10^6 cells after coincubation with specific transport inhibitors (15 mmol/L) for 4 min: BCH as competitive inhibitor of system L, MeAIB as competitive inhibitor of system A, and MeAIB plus serine as competitive inhibitor of system ASC. (B) Uptake of ^{11}C-MCYS per 10^6 cells at different concentrations (μmol/L) of MCYS in incubation medium.

Tracer Uptake in Mice

The biodistribution data of ^{11}C-MCYS in normal mice are summarized in Table 1. The highest uptake of ^{11}C-activity in all tissues was found to exceed 0.6 %ID/g at 5 min after injection. The liver had the highest uptake of ^{11}C-MCYS, next to the stomach wall and heart, and the brain had relatively low uptake of ^{11}C-MCYS. Low uptake levels of ^{11}C-MCYS in normal tissues were observed at 30 min after injection The radioactivity in the blood was rapidly decreased from 0.94 ± 0.12 %ID/g at 5 min after injection to 0.17 ± 0.02 %ID/g at 60 min after injection. No elevated organ uptake of ^{11}C-MCYS in the organs sampled was found at 30 min after injection. At 60 min after injection, brain and muscle showed the lowest uptake. Uptake of ^{11}C-MCYS in the brain did not exceed 0.60 %ID/g at any time during the observation except 5 min after injection. Uptake of ^{11}C-MCYS into the brain was slow and decreased slightly at 30 min after injection.

Incorporation of ^{11}C-MCYS into Proteins

Protein-bound activity of ^{11}C-MCYS in brain, pancreas, tumor, and blood samples demonstrated less than 1% of the radioactivity to be in the acid-precipitable fraction and almost all the radioactivity to be in the acid solution fraction (Fig. 4). Thus, almost no incorporation of ^{11}C-MCYS into proteins was observed. Also, high-performance liquid chromatography analysis of plasma samples, brain, pancreas, and tumor tissue at 30 min after injection showed that the activity was completely eluted in the low-molecular-weight fraction. All activity extracted from tissue homogenates, spiked with MCYS, and analyzed on high-performance liquid chromatography was coeluted with the cold standard. In all cases, the major radioactive component, corresponding to parent ^{11}C-MCYS, eluted at a retention time of 2.0 min. In the acid solution fractions from brain, pancreas, tumor, and blood samples, parent ^{11}C-MCYS comprised more than 90% of the total radioactivity. These results showed that ^{11}C-MCYS was metabolically stable in vivo.

PET Studies

Whole-body imaging provided the consistent distribution data (Suppl. Fig. 2) obtained from the tissue dissection assays. As for uptake into the inoculated tumors, high ^{18}F-FDG and ^{11}C-MCYS uptake (Suppl. Figs. 2A and 2C) and relatively low ^{11}C-MET uptake (Suppl. Fig. 2B) were found, and tumor-to-muscle ratios were highest for ^{11}C-MCYS uptake. Similarly, high ^{18}F-FDG and ^{11}C-MET uptake was observed in the inflammation group. In contrast, low ^{11}C-MCYS uptake was observed in inflammatory tissue. The uptake percentages of ^{11}C-MCYS, ^{18}F-FDG, and ^{11}C-MET in tumor, inflammatory lesions, and muscle at 60 min after injection are shown in Table 2.

As for the patient with postoperative grade IV glioma, MRI showed a new abnormal enhancing lesion (Fig. 5), and

TABLE 1
Biodistribution of ^{11}C-MCYS in Normal Mice After Intravenous Injection

Organ	5 min	10 min	20 min	30 min	60 min
Blood	1.03 ± 0.12	0.71 ± 0.08	0.38 ± 0.07	0.21 ± 0.09	0.17 ± 0.02
Brain	0.72 ± 0.06	0.60 ± 0.09	0.33 ± 0.06	0.18 ± 0.07	0.13 ± 0.04
Heart	0.94 ± 0.15	0.89 ± 0.08	0.68 ± 0.06	0.40 ± 0.05	0.31 ± 0.06
Lung	0.91 ± 0.11	0.72 ± 0.12	0.42 ± 0.30	0.38 ± 0.30	0.23 ± 0.05
Liver	1.97 ± 0.12	1.38 ± 0.10	1.06 ± 0.09	0.86 ± 0.12	0.53 ± 0.14
Kidney	0.89 ± 0.09	0.62 ± 0.08	0.58 ± 0.08	0.32 ± 0.06	0.29 ± 0.05
Stomach wall	0.99 ± 0.15	0.87 ± 0.10	0.62 ± 0.09	0.44 ± 0.07	0.20 ± 0.04
Small intestine	0.92 ± 0.32	0.75 ± 0.19	0.63 ± 0.23	0.46 ± 0.07	0.32 ± 0.14
Muscle	0.61 ± 0.04	0.35 ± 0.08	0.28 ± 0.05	0.17 ± 0.06	0.14 ± 0.02

Data are average %ID/g ± SD (n = 5).

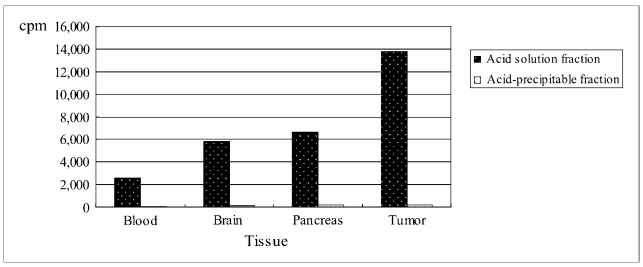

FIGURE 4. Radioactivities contained in acid solution and acid-precipitable fractions at 30 min after injection.

^{18}F-FDG PET showed heterogeneous hypometabolism in the right temporal lobe (Fig. 5B). However, ^{11}C-MCYS PET showed markedly high uptake in the lesion (Fig. 5A), and histopathologic examination confirmed tumor recurrence.

DISCUSSION

^{11}C-MCYS, as an analog of ^{11}C-MET, can efficiently be produced by a method similar to that for ^{11}C-MET and exhibits similar biologic activity (*14,18*). MCYS is a naturally occurring inexpensive water-soluble compound found abundantly in cabbage, garlic, and turnips that has antioxidative and antiinflammatory properties and no adverse effects (*19–21*). Therefore, evaluation of ^{11}C-MCYS and its automated synthesis is important.

Tumor uptake is thought to reflect increased active transport and protein synthesis (*3,22*). Most amino acids are taken up by tumor cells through the sodium-independent L-type amino acid transporter system and the sodium-dependent transporter systems A and ASC (*16*). Several positron-labeled naturally occurring amino acids show protein incorporation (e.g., L-1-^{11}C-tyrosine and, partly, ^{11}C-MET) (*3,22*), and labeled non–protein-composition amino acids show amino acid transport (e.g., ^{18}F-FET and, partly, 2-^{18}F-fluoro-L-phenylalanine) (*3,22*). For example, ^{18}F-FET is not incorporated into proteins with relatively stable metabolism in vivo, and ^{18}F-FET uptake is mediated through system L (*23*). Like ^{18}F-FET, ^{11}C-MCYS is a non–protein-composition amino acid tracer with relative metabolic stability in vivo and not incorporated into proteins, confirmed by ^{11}C-MCYS incorporation and metabolism experiments in this work. In addition, we found that a specific transport of ^{11}C-MCYS in Hep1–6 cells was mediated mainly by system L, with almost no involvement of systems A and ASC, and that ^{11}C-MCYS uptake was not affected by the presence of Na^+. These findings are consistent with the fact that system L has no requirement for sodium and energy sources, in contrast to systems A and ASC (*24*). However, ^{11}C-MET is an ^{11}C-labeled naturally occurring amino acid that can be used to estimate muscle protein synthetic rates (*25*) and also generates substantial amounts of nonprotein metabolites in vivo (*22*). Interestingly, the rapid initial uptake of ^{11}C-MET in tissues mainly reflects amino acid transport, rather than protein synthesis (*3*). Like the uptake mechanism of ^{11}C-MCYS, ^{11}C-MET transport is usually mediated through system L, with minor contributions from systems A and ASC (*22*).

Currently, 4 subtypes of the sodium-independent L-type amino acid transporter (LAT) have been reported: LAT1, LAT2, LAT3, and LAT4 (*26,27*). The well-known LAT1 seems to be an excellent and promising target for molecular imaging and shows increased transport activity in many cancer cells via transporting neutral amino acids, including methionine (*27*). Higher LAT1 protein expression levels in high-grade glioma cells than in low-grade gliomas and normal brain tissue have been found (*28*), as has LAT1 expression in hepatocarcinoma cells (*29*). ^{11}C-MET transport may be increased by an increased number of microvessels combined with a higher density or activity of LAT1 in the tumor endothelial cells in high-grade gliomas (*28*). ^{18}F-FET can be selectively transported by LAT2 and can differentiate tumor from inflammation, possibly contributing to increased amino acid transport and no expression of LAT2 in inflammatory tissue (*23*). In this work, high uptake of ^{11}C-MCYS in hepatoma tissue and low ^{11}C-MCYS uptake in inflammatory tissue are possibly associated with the increased amino acid transport of ^{11}C-MCYS and its lack of incorporation into protein. Thus, we can assume that ^{11}C-MCYS uptake is transported mainly by LAT1, LAT2, or both. PET of the glioma patient showed high ^{11}C-MCYS uptake in tumor tissue and low tracer uptake in normal brain tissue, further supporting this assumption.

TABLE 2
Uptake of ^{11}C-MCYS, ^{18}F-FDG, and ^{11}C-MET in Tumor, Inflammatory Lesion, and Muscle at 60 Minutes After Injection in Tumor-Model Mice and Inflammation-Model Mice

Tissue	^{11}C-MCYS	^{18}F-FDG	^{11}C-MET
Tumor	4.58 ± 0.65	4.32 ± 0.47	3.03 ± 0.79
Inflammation	1.02 ± 0.18	3.30 ± 0.23	1.62 ± 0.68
Muscle	0.63 ± 0.05	0.85 ± 0.13	0.71 ± 0.09
Tumor-to-muscle ratio	7.27	5.08	4.26
Inflammation-to-muscle ratio	1.62	3.88	2.28

Mice (n = 5) were killed at 60 min after injection; tissue samples were rapidly removed, and weight and radioactivity were measured. Data are average %ID/g ± SD (n = 5), or ratio.

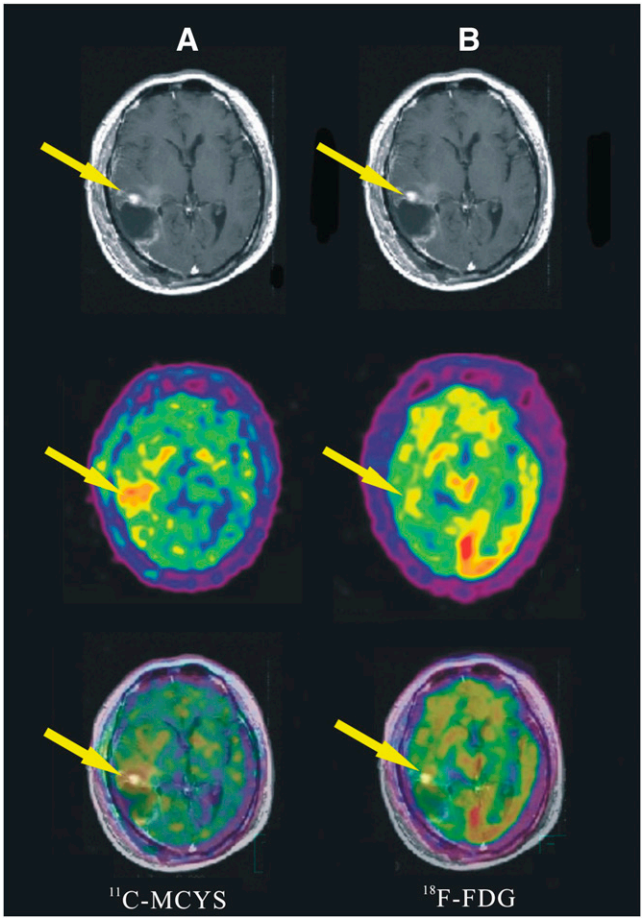

FIGURE 5. MRI, PET, and coregistered PET/MRI images from top to bottom, respectively, in 45-year-old man with history of attempted resection of grade IV glioma. (A) ^{11}C-MCYS PET illustrates obvious hypermetabolic lesion as depicted by gadolinium-enhanced MRI (arrow), suggesting predominant high-grade tumor recurrence, which was confirmed on histopathology. (B) ^{18}F-FDG PET shows slightly low uptake in patch-shaped heterogeneous hypometabolic area in right temporal lobe (arrow).

The biodistribution demonstrated a continually increasing accumulation of ^{11}C-MCYS in tumor up to 30 min after injection, relatively low uptake of ^{11}C-MCYS in brain and muscle during the entire observation time, and rapid radioactivity clearance from most tissues. Thus, fast tumor uptake kinetics and low accumulation of ^{11}C-MCYS in the brain and most tissues showed that ^{11}C-MCYS is a potential amino acid PET tracer for imaging of cerebral and peripheral tumors. The good scan time was within 30 min after injection of ^{11}C-MCYS.

Several investigators have shown high accumulation of ^{18}F-FDG in turpentine-induced inflammatory tissue (*12*) and *Staphylococcus aureus*–inoculated inflammation models (*30*). This study found high uptake of ^{18}F-FDG and ^{11}C-MET and low uptake of ^{11}C-MCYS in the turpentine-induced inflammatory tissues, whereas high uptake of ^{18}F-FDG and ^{11}C-MCYS and relatively low uptake of ^{11}C-MET were found in Hepa1–6 tumors. These results show that ^{11}C-MCYS has advantages over ^{18}F-FDG and ^{11}C-MET in the differentiation of tumor from inflammation. Furthermore, in the patient with brain glioma, the high uptake of ^{11}C-MCYS in contrast to the very low uptake of ^{18}F-FDG indicated that ^{11}C-MCYS is superior to ^{18}F-FDG for malignant glioma imaging. However, all these results require further confirmation before clinical application is possible.

CONCLUSION

The automated synthesis of ^{11}C-MCYS is easy to perform. Our initial study results show that ^{11}C-MCYS is transported by the specific amino acid transport system L and is not incorporated into proteins. ^{11}C-MCYS is superior to ^{18}F-FDG and ^{11}C-MET in the differentiation of tumor from inflammation. ^{11}C-MCYS PET is more sensitive and specific than ^{18}F-FDG PET in the detection of cancer. Therefore, ^{11}C-MCYS may be potentially better than ^{11}C-MET as an amino acid PET tracer for tumors, but further confirmation is needed in clinical studies.

ACKNOWLEDGMENTS

We thank Xiangsong Zhang and Zhenhua Gao for assistance with this work. This work was supported by the National Natural Science Foundation (grant 30970856), the National High Technology Research and Development Program of China (program 863, grant 2008AA02Z430), and Sun Yat-Sen University (grant 18901205).

REFERENCES

1. Tang GH. Positron emission tomography imaging and drug development. *Acta Pharmacol Sin.* 2001;36:470–474.
2. Heiss P, Mayer S, Herz M, Wester HJ, Schwaiger M, Senekowitsch-Schmidtke R. Investigation of transport mechanism and uptake kinetics of O-(2-^{18}F-fluoroethyl)-L-tyrosine in vitro and in vivo. *J Nucl Med.* 1999;40:1367–1373.
3. Laverman P, Boerman OC, Corstens FHM, Oyen WJG. Fluorinated amino acids for tumour imaging with positron emission tomography. *Eur J Nucl Med Mol Imaging.* 2002;29:681–690.
4. Kubota K. From tumor biology to clinical PET: a review of positron emission tomography (PET) in oncology. *Ann Nucl Med.* 2001;15:471–486.
5. Sasaki M, Kuwabara Y, Yoshida T, et al. Comparison of MET-PET and FDG-PET for differentiation between benign lesions and malignant tumors of the lung. *Ann Nucl Med.* 2001;15:425–431.
6. Yasukawa T, Yoshikawa K, Aoyagi H, et al. Usefulness of PET with ^{11}C-methionine for the detection of hilar and mediastinal lymph node metastasis in lung cancer. *J Nucl Med.* 2000;41:283–290.
7. Maeda Y, Oguni H, Saitou Y, et al. Rasmussen syndrome: multifocal spread of inflammation suggested from MRI and PET findings. *Epilepsia.* 2003;44:1118–1121.
8. Ishiwata K, Vaalburg W, Elsinga PH, Paans AMJ, Woldring MG. Comparison of L-1-^{11}C-methionine and L-methyl-[^{11}C]methionine for measuring in vivo protein synthesis rates with PET. *J Nucl Med.* 1988;29:1419–1427.
9. Lee TS, Ahn SH, Moon BS, et al. Comparison of ^{18}F-FDG, ^{18}F-FET and ^{18}F-FLT for differentiation between tumor and inflammation in rats. *Nucl Med Biol.* 2009;36:681–686.
10. Hamacher K, Coenen HH. Efficient routine production of the ^{18}F-labelled amino acid O-(2-[^{18}F]fluoroethyl)-l-tyrosine. *Appl Radiat Isot.* 2002;57:853–856.
11. Pascali C, Bogni A, Iwata R, Decise D, Crippa F, Bombardieri E. High efficiency preparation of L-[S-methyl-^{11}C]methionine by on column [^{11}C]methylation on C18 Sep-Pak. *J Labelled Comp Radiopharm.* 1999;42:715–724.
12. Yamada S, Kubota K, Kubota R, Ido T, Tamahashi N. High accumulation of fluorine-18-fluorodeoxyglucose in turpentine-induced inflammatory tissue. *J Nucl Med.* 1995;36:1301–1306.

13. Hamacher K, Coenen HH, Stocklin G. Efficient stereospecific synthesis of no-carrier-added 2-[^{18}F]-fluoro-2-deoxy-D-glucose using aminopolyether supported nucleophilic substitution. *J Nucl Med.* 1986;27:235–238.
14. Tang GH, Wang MF, Tang XL, Luo L, Gan MQ. Automated synthesis of (S-[^{11}C]-methyl)-L-methionine and (S-[^{11}C]-methyl)-L-cysteine by on-column [^{11}C] methylation. *Nucl Technol.* 2004;26:77–83.
15. Tang GH, Tang XL, Wang MF, Guo XJ. High efficient automated synthesis of 2-[^{18}F]-fluoro-2-deoxy-D-glucose. *Nucl Technol.* 2006;29:531–536.
16. Langen KJ, Jarosch M, Muhlensiepen H, et al. Comparison of fluorotyrosine and methionine uptake in F98 rat gliomas. *Nucl Med Biol.* 2003;30:501–508.
17. Langen KJ, Muhlensiepen H, Schmieder S, et al. Transport of cis- and trans-4-[^{18}F]fluoro-L-proline in F98 gliomas cells. *Nucl Med Biol.* 2002;29:685–692.
18. Deng HF, Tang GH, Wang HL, et al. Radiosynthesis and evaluation of ^{11}C-CYS as an oncologic PET tracer [abstract]. *J Nucl Med.* 2010;51(suppl 2):102P.
19. Wassef R, Haenold R, Hansel A, Brot N, Heinemann SH, Hoshi1 T. Methionine sulfoxide reductase A and a dietary supplement S-methyl-L-cysteine prevent Parkinson's-like symptoms. *J Neurosci.* 2007;27:12808–12816.
20. Yeh YY, Liu L. Cholesterol-lowering effect of garlic extracts and organosulfur compounds: human and animal studies. *J Nutr.* 2001;131:989S–993S.
21. Hsu CC, Huang CN, Hung YC, Yin MC. Five cysteine-containing compounds have antioxidative activity in Balb/cA mice. *J Nutr.* 2004;134:149–152.
22. Jager PL, Vaalburg W, Prium J, de Vries EGE, Langen KJ, Piers DA. Radiolabeled amino acid: basic aspects and clinical applications in oncology. *J Nucl Med.* 2001;42:432–445.
23. Langen KJ, Hamacher K, Weckesser M, et al. O-(2-[^{18}F]fluoroethyl)-L-tyrosine: uptake mechanisms and clinical applications. *Nucl Med Biol.* 2006;33: 287–294.
24. Tovar AR, Tews JK, Torres N, Harper AE. Neutral amino acid transport into rat skeletal muscle: competition, adaptive regulation, and effects of insulin. *Metabolism.* 1991;40:410–419.
25. Fischman AJ, Yu YM, Livni E, et al. Muscle protein synthesis by positron-emission tomography with L-[methyl-^{11}C]methionine in adult humans. *Proc Natl Acad Sci USA.* 1998;95:12793–12798.
26. McConathy J, Goodman MM. Non-natural amino acids for tumor imaging using positron emission tomography and single photon emission computed tomography. *Cancer Metastasis Rev.* 2008;27:555–573.
27. Haase C, Bergmann1 R, Fuechtner F, Hoepping A, Pietzsch J. L-type amino acid transporters LAT1 and LAT4 in cancer: uptake of 3-O-methyl-6-^{18}F-fluoro-L-dopa in human adenocarcinoma and squamous cell carcinoma in vitro and in vivo. *J Nucl Med.* 2007;48:2063–2071.
28. Okubo S, Zhen H, Kawai N, Nishiyama Y, Haba R, Tamiya T. Correlation of L-methyl-^{11}C-methionine (MET) uptake with L-type amino acid transporter 1 in human gliomas. *J Neurooncol.* 2010;99:217–225.
29. Fuchs BC, Bode BP. Amino acid transporters ASCT2 and LAT1 in cancer: partners in crime? *Semin Cancer Biol.* 2005;15:254–266.
30. Kaim AH, Weber B, Kurrer MO, et al. ^{18}F-FDG and ^{18}F-FET uptake in experimental soft tissue infection. *Eur J Nucl Med Mol Imaging.* 2002;29: 648–654.